Progress In Electromagnetics Research C, Vol. 57, 25–34, 2015

A Novel Tri-Band Hexagonal Microstrip Patch Antenna Using Modified Sierpinski Fractal for Vehicular Communication

Tapas Mondal[1, *], Susamay Samanta[1], Rowdra Ghatak[2], and Sekhar R. Bhadra Chaudhuri[3]

Abstract—The present paper analyses and documents the merits of incorporating fractal design in microstrip antenna intended to be mounted on and integrated into the design of smart vehicles. A novel design is proposed for a compact tri-band hexagonal microstrip antenna to be integrated with the body of a smart vehicle for short range communication purpose in an Intelligent Transport System (ITS). This antenna can be used at 1.575 GHz of GPS L1 band for vehicle to roadside communication, at 3.71 GHz of mobile WiMAX band (IEEE 802.16e-2005) for blind spot detection and at 5.9 GHz of DSRC band (IEEE 802.11p) for vehicle to vehicle communication. At 3.71 GHz, the two major lobes of the antenna radiation beam, tilted by 35° on both sides from its broadside direction, help the vehicle to detect blind spots efficiently. The largest dimension of the proposed antenna corresponds to the lowest resonating frequency, 1.575 GHz. Compared to the conventional hexagonal patch, the modified Sierpinski fractal proposed herein reduces the overall area, at 1.575 GHz, by 75%, with 5.2 dBi gain. In comparison with other popular fractals, the proposed fractal structure achieves demonstrably better antenna miniaturization. When the antenna is mounted on the vehicle, considered an electromagnetically larger object, the simulated and on-vehicle experimental results show antenna gains of more than 5.5 dBi at 1.575 GHz, 8 dBi at 3.71 GHz and 9 dBi at 5.9 GHz in the desired direction with negligible amount of electromagnetic interference inside the car.

1. INTRODUCTION

Complex transportation systems and smart vehicles emerging due to the rapid evolution of technology require reliable, low cost, high performance and low delay traffic safety applications. But there exist significant challenges to the development of such applications. The high speed of vehicles and harsh dynamic communication environments are typical instances of such challenges. Most of the present conventional vehicular safety equipments such as shadow or edge feature detectors [1] and side view cameras [2] have performance limitations in the presence of mist, fog and bad weather. Solid state infra-red detectors [3] are highly expensive. Mechanically controlled devices like dynamic angling side view mirrors [4] are easily broken or damaged by everyday use.

These technical and economical challenges have created an opportunity for the application of radio frequency in this field and hence the use of antennas in the context of vehicular communication has gained in prominence. Recently, the design of miniaturized fractal antennas capable of providing multiple resonant frequencies has received much attention due to ease of installation on vehicles and aerodynamic compatibility [5]. Several research papers have proposed novel antenna design techniques based on fractal geometry [6–8], showing how proper selection of fractal geometry can help reduce the

Received 11 February 2015, Accepted 30 March 2015, Scheduled 10 April 2015

* Corresponding author: Tapas Mondal (tapas2k@gmail.com).

[1] ECE Department, Dr. B. C. Roy Engineering College, Durgapur, West Bengal, India. [2] Microwave and Antenna Research Laboratory, Department of ECE, National Institute of Technology Durgapur, West Bengal, India. [3] Department of E & TCE, Indian Institute of Engineering Science and Technology, Shibpur, West Bengal, India.

overall antenna size and, simultaneously, ensure multi-band operation. Fractals are set of geometrical structures featuring two main properties — self-similarity and space filling [9]. The implementation of the space filling property of fractal geometry results in smaller antenna size [10] and the self-similarity property ensures similar antenna radiation characteristics through several bands. The Sierpinski carpet fractal [11] is one of the popular fractal design implemented in microstrip antenna structures for multiband operations along with antenna miniaturization.

The present paper proposes a novel tri-band microstrip patch antenna for short range vehicular communications. Its design is based on a multi-layered structure that incorporates a hexagonal Sierpinski fractal geometry for the patch. The performance of the patch is analysed and compared to a hexagonal patch without fractal configuration to assess antenna size reduction in the modified design. A study is also conducted to analyse if the non-radiating vacant space at the center of the proposed hexagonal patch can be utilised efficiently. In this sense, a smaller patch yet, of similar configuration, is introduced at the center of the first patch. Simulation runs of the combined structure reveal the tri-band behaviour of the antenna. The proposed antenna can operate at 1.575 GHz of the GPS L1, 3.71 GHz of WiMAX, and 5.9 GHz of DSRC bands. The performance of the present antenna element is estimated by both numerical simulations and experimental measurements. The performance of the element after mounting on a vehicle is also studied. The analysis also includes a numerical comparison between the proposed antenna and many of the existing compact multi-band patch solutions.

In this paper, a comprehensive design of the proposed hexagonal microstrip antenna using a modified Sierpinski fractal structure is discussed in Section 2. In Section 3 placement of the antenna on the body of a vehicle is illustrated. In Section 4 the key results and accompanying discussions are displayed, followed by the conclusion in Section 5.

2. ANTENNA DESIGN

2.1. Formulation of Hexagonal Patch Dimension from Circular Patch Dimension

The formulation of the resonance frequency of a hexagonal microstrip patch antenna (HMSA) can be obtained from the resonance frequency equation of the circular microstrip patch antenna (CMSA) [12] by equating the respective areas as shown in Fig. 1. The resonance frequency of the hexagonal microstrip patch antenna is given by (1).

$$f_r = \frac{\chi_{mn} c}{5.7138 s \sqrt{\epsilon_{reff}}} \tag{1}$$

where,
$\chi_{mn} = \chi_{11}$ (for TM_{11} mode) $= 1.84118$;
$\chi_{mn} = \chi_{21}$ (for TM_{21} mode) $= 3.05424$;
and ϵ_{reff} is the effective dielectric constant of the substrate material.

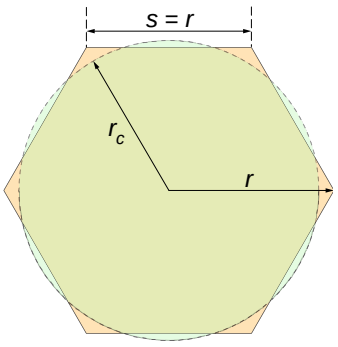

Figure 1. A circle and a hexagon with equal areas.

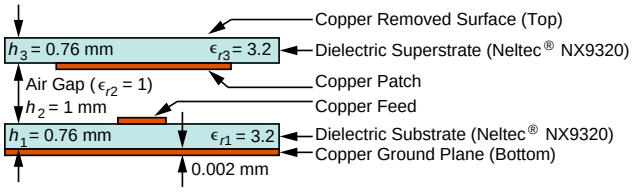

Figure 2. Multi-layered structure.

2.2. Choice of Substrate and Multi-Layered Structure

The substrate, Neltec® NX9320 with dielectric constant ϵ_r 3.2, thickness h 0.76 mm and dielectric loss tangent $\tan\delta$ 0.0024 has been taken for this design. The thickness of the copper clad is 0.002 mm. For the enhancement of the antenna gain, a multi-layered structure [12, 17] as illustrated in Fig. 2 is proposed. The topmost copper layer is etched and removed. Neltec® NX9320, as specified earlier, is also used as the superstrate.

An air gap of 1 mm is created between the upper and lower dielectric substrates by using nylon spacer. The copper cladding of the lower side of the superstrate is used for the construction of the proposed hexagonal patch antenna. The basic microstrip antenna is designed and placed at a height of 1.76 mm from the ground plane. ϵ_{r1}, ϵ_{r2} and ϵ_{r3} are the values of dielectric constant and h_1, h_2 and h_3 are the values of the thickness of layers 1, 2 and 3 respectively as shown in Fig. 2. Therefore, the value of the effective dielectric constant ϵ_{reff} of this 3-layer microstrip structure [13] is obtained as 2.02.

2.3. Dimension of Hexagonal Patch without Fractal

The process starts with designing a plain hexagonal patch supposed to operate at 1.575 GHz. Using (1), the side length of such a regular hexagonal microstrip antenna (HMSA) is computed to be 43.18 mm. This side length s is the average current path L length for the hexagonal patch antenna. Hence,

$$L = s = 43.18\,\text{mm} \tag{2}$$

Analysis has been carried out to reduce the size of the individual elements by incorporating hexagonal Sierpinski carpet fractal geometry into the antenna structure.

2.4. Dimension of Hexagonal Patch with Modified Sierpinski Fractal

The Sierpinski carpet fractal is introduced in the hexagonal patch by including successive hexagonal ring structures into the patch. For further improvement in miniaturization, the structure is modified by etching out successive T-shaped slots at angles 30°, 90°, 150°, 210°, 270° and 330°, as portrayed in Fig. 3(a), representing the general structure of the proposed hexagonal patch antenna with modified Sierpinski carpet fractal.

It is important to observe the surface current distribution for evaluating the patch resonance frequency by measuring the length of the current path between its nulls [14]. As an example, Fig. 3(b) illustrates the vector current paths across the surface of the modified Sierpinski fractal antenna resonating at 1.575 GHz.

On rigorous experimentation, it is observed from the surface current distribution that the average current path L length for the proposed structure can be governed by the following novel empirical

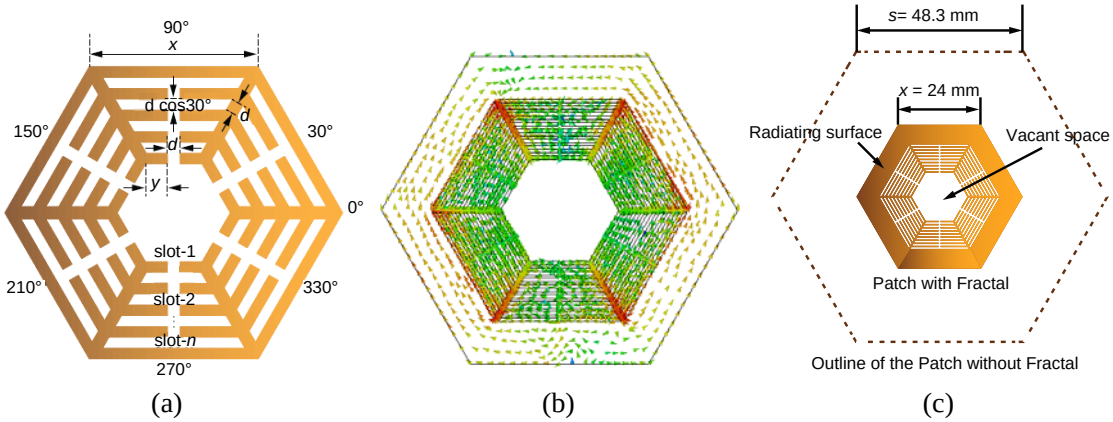

Figure 3. (a) General Structure of hexagonal patch with modified Sierpinski carpet fractal. (b) Vector current paths for evaluation of resonance frequency of the patch. (c) Surface area reduction using the proposed fractal.

equation:

$$L = x + 2\,(y + nd + nd\cos 30^\circ) \tag{3}$$

The dimensions x, y and d are indicated in the general structure as portrayed in Fig. 3(a). n is the number of slot rings etched out from the centre to the side of the hexagonal patch in a radial direction. According to Sierpinski fractal theory, in this case, the side length of the innermost hexagon should be equal to of the $\frac{1}{3}rd$ of the outermost hexagon. Again as the average current path length is constant for a given frequency, it is true that $L = s$. Therefore,

$$s = \frac{4x}{3} + d(3.73205n - 1) \tag{4}$$

Hence, it is clear from (4) that the side length x of the hexagonal patch antenna with modified Sierpinski fractal is always less than the side length s of the hexagonal patch without fractal.

By further parametric studies, optimization and simulation in Ansys HFSS$^{\text{TM}}$ it has been found that, $L_1 = s_1 = 48.30\,\text{mm}$, $x_1 = 24\,\text{mm}$, $n_1 = 9$ and $d_1 = 0.52\,\text{mm}$ suffice to make the antenna operate at 1.575 GHz as shown in Fig. 3(c). The overall radiating surface area of the patch is reduced by 75%.

The non radiating vacant space at the center of the patch as shown in Fig. 3(c) is utilized by introducing a smaller patch of length 5.25 mm with similar modified Sierpinski fractal structure as illustrated in Fig. 4. The dimensions $L_2 = s_2 = 11.56\,\text{mm}$ $x_2 = 5.25\,\text{mm}$ and $d_2 = 0.39\,\text{mm}$ suffice for this smaller patch to resonate at 5.9 GHz.

The two concentric hexagonal patches individually contribute to the lower resonating frequency 1.575 GHz and the upper resonating frequency 5.9 GHz respectively. But, the third resonance at 3.71 GHz is observed due to the combined electromagnetic effect of these two concentric resonating structures which is discussed in Section 4. Hence, the average current path corresponding to 3.71 GHz of this structure cannot be specifically governed by the Formula (3) or (4) which are proposed for a single hexagonal fractal structure only. Further, to demonstrate the accuracy of the proposed empirical Formulae (3) and (4), the calculated average current path lengths using (1) for three sample frequencies are tabulated in Table 1 along with the average current path lengths as obtained from the simulation

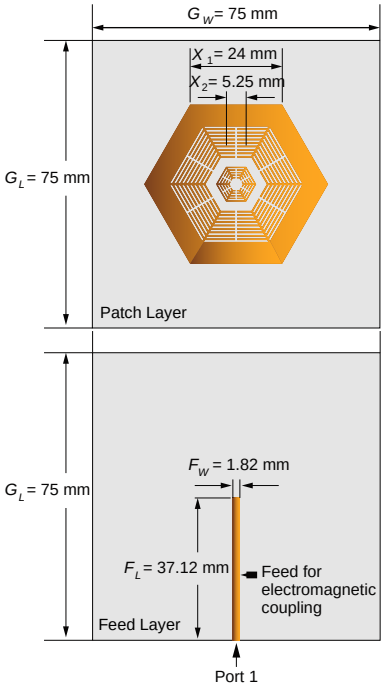

Figure 4. Layout of the antenna geometry.

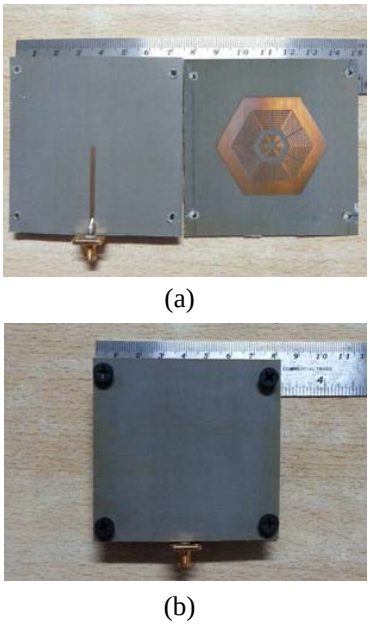

Figure 5. Snapshots of the fabricated antenna. (a) Unfolded layers. (b) Top view of the fabricated antenna.

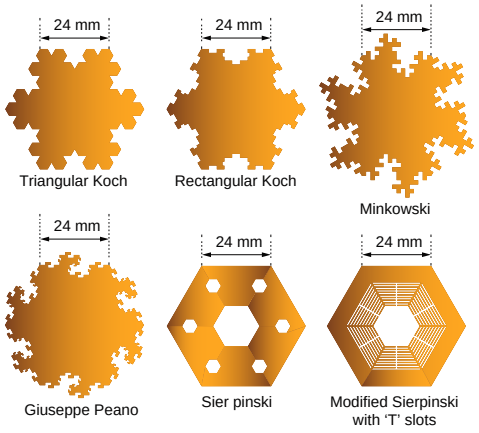

Figure 6. Different hexagonal fractal antennas.

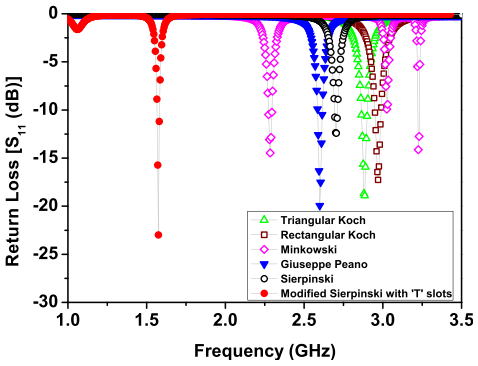

Figure 7. Return loss vs. frequency plot.

Table 1. Accuracy of the proposed formulae for different resonance frequencies.

Resonance Frequency (GHz)	$L_{calculated}$ (mm)	$L_{proposed}$ (mm)	Percentage of error
1.575	43.18	48.30	11.86%
5.9	11.528	11.566	0.32%
7.2	9.4468	9.4472	0.42%

and optimization. It can be clearly observed that as the resonance frequency increases, the level of accuracy of the proposed empirical formulae improves considerably.

The dimensions of the finite dielectric area and finite ground plane area around the patch are taken as 75 mm × 75 mm. The width of the microstrip feed line F_W is 1.82 mm, and the length of the feed line F_L is 37.12 mm. The snapshots of the fabricated antenna are framed in Fig. 5.

2.5. Investigation of Miniaturization Performance of the Proposed Fractal Structure

It is necessary to investigate the effectiveness of the proposed fractal structure for antenna miniaturization application. The common popular fractal structures such as Triangular Koch [15], Rectangular Koch [17], Minkowski [16], Giuseppe Peano [17] and normal Sierpinski [11] up to second iteration along with the proposed modified Sierpinski are incorporated within the surface of hexagonal patches of fixed side length 24 mm as illustrated in Fig. 6. The plots of the comparative return loss S_{11} (dB) against frequency are compared in Fig. 7.

From Fig. 7 it can be observed that the hexagonal patch antenna incorporating the proposed fractal structure gives response at 1.575 GHz. But, the other hexagonal fractal antennas having equal length as of the proposed hexagonal fractal structure have responses at higher frequencies. Therefore, the proposed modified Sierpinski fractal is more effective than the other popular fractals in achieving antenna miniaturization.

3. PLACEMENT OF THE ANTENNA ON THE VEHICLE

A reasonably complete study and observation of the radiation characteristics of the antenna is impossible without placing it on the body of a vehicle since it acts as an infinite ground plane unlike the antenna itself whose ground plane is finite. For the respective analysis, a car model is designed in Ansys HFSS^{TM} in which conducting material is assigned to the hood, roof, trunk, doors and quarter panel whereas the bumpers and wheels are modelled as layered impedance due to their hard rubber and polyester constituents as shown in Fig. 8. As the dimension of the vehicle is very large with respect to the operating wavelengths of the proposed antenna, a very high-end computational domain is required

Table 2. Time and memory usage by the on-vehicle antenna simulation in Ansys HFSS^{TM} at 5.9 GHz.

Task	Real Time (hh : mm : ss)	CPU Time (hh : mm : ss)	Memory
Mesh (surface init)	0 : 00 : 09	0 : 00 : 09	141 M
Mesh (surface translation)	0 : 00 : 01	0 : 00 : 01	90.6 M
g3dm_simprove	0 : 00 : 04	0 : 00 : 04	99.7 M
Mesh (surface lambda)	0 : 00 : 17	0 : 00 : 17	402 M
Get external near field	0 : 00 : 20	0 : 00 : 00	0 K
Simulation setup	0 : 00 : 04	0 : 00 : 04	505 M
Solver Preprocess	0 : 00 : 37	0 : 00 : 37	2.26 G
Matrix Assembly	0 : 07 : 21	0 : 07 : 21	3.65 G
Matrix Solve	2 : 35 : 18	2 : 35 : 10	13.7 G
Post-process solution	0 : 00 : 24	0 : 00 : 24	13.7 G

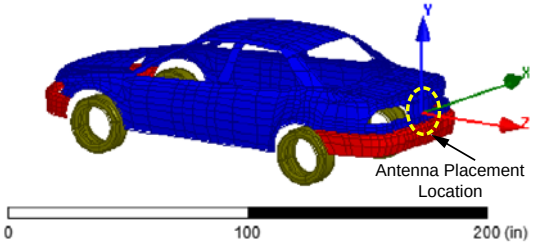

Figure 8. Simulation model of the entire vehicle.

Figure 9. On-vehicle experimental set-up.

to simulate the antenna structure after the antenna is placed on the vehicle. In Table 2, the time and the memory (RAM) usage for the different tasks involved in simulation of the proposed antenna at 5.9 GHz along with the vehicle are enlisted. It has been extracted from the HFSS-IE solution data. The on-vehicle experimental set-up to measure the radiation pattern of the antenna is framed in Fig. 9.

4. RESULTS AND DISCUSSIONS

This section presents the results provided by simulations and discusses the results obtained to study the effect of fractal geometry, multi-layer structure, vehicle body and presence of another vehicle as scattering object in separate sub-sections.

4.1. Simulation of the Solid Hexagonal Patch without Fractal

The scattering parameter, radiation pattern and efficiency of the solid hexagonal patch without fractal corresponding to 1.575 GHz and 5.9 GHz are simulated in Ansys HFSS^{TM}. At 1.575 GHz, the solid hexagonal patch has been found to operate with an impedance bandwidth of 10.67 MHz as shown in Fig. 10(a), gain of 7.84 dB as shown in Fig. 12(a) and radiation efficiency of 88.87%. At 5.9 GHz, a similar but smaller solid patch has been found to operate with an impedance bandwidth of 162 MHz Fig. 10(c), gain of 7.96 dB Fig. 12(c) and radiation efficiency of 90.10%.

4.2. Simulation and Experimentation of the Proposed Fractal Antenna

The scattering parameter is simulated in Ansys HFSS^{TM} and then it is measured by Agilent Technologies Vector Network Analyzer of model No. N5320A (10 MHz to 20 GHz). The proposed antenna has been found to operate at 1.575 GHz with 16.8 MHz 10 dB impedance bandwidth; at 3.71 GHz with 77 MHz 10 dB impedance bandwidth and at 5.9 GHz with 154 MHz 10 dB impedance bandwidth. The compared return loss S_{11} (dB) is shown in Fig. 10. The vector current distributions across the surface of the antenna at these three frequencies are illustrated in Fig. 11 which clearly reflects the individual

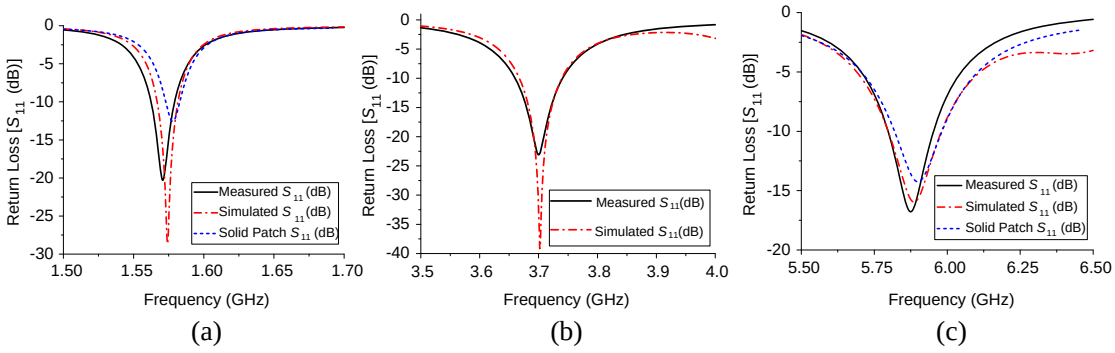

Figure 10. Return loss of the antenna element. (a) 1.575 GHz. (b) 3.71 GHz. (c) 5.9 GHz.

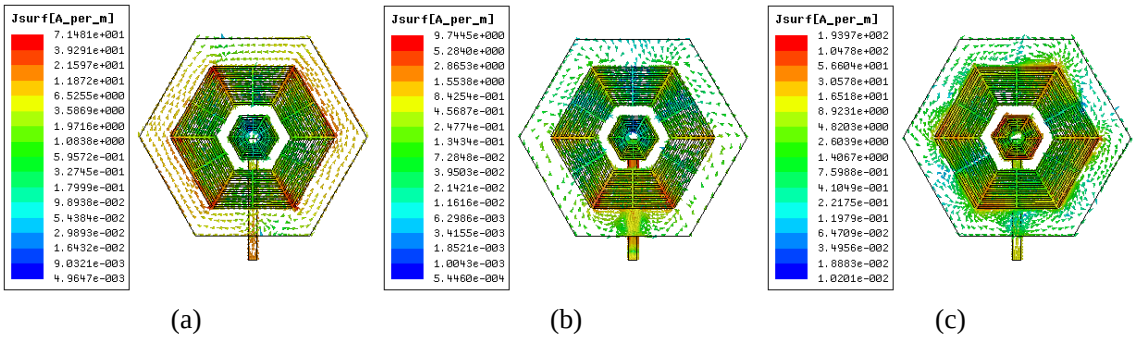

Figure 11. Vector current distribution. (a) 1.575 GHz. (b) 3.71 GHz. (c) 5.9 GHz.

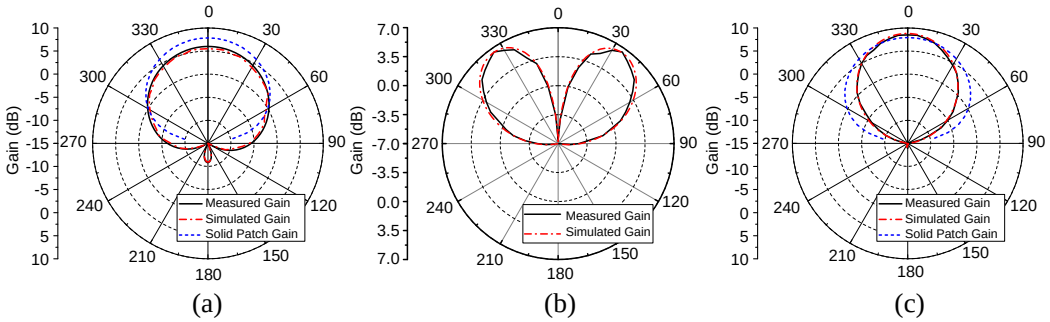

Figure 12. 2D radiation patterns of the antenna element (at ϕ= 0° plane). (a) 1.575 GHz. (b) 3.71 GHz. (c) 5.9 GHz.

contributions of the two concentric patches to generate resonance at 1.575 GHz and 5.9 GHz along with the combined electromagnetic effect of these two structures to generate the third resonance at 3.71 GHz.

The radiation patterns at 1.575 GHz, 3.71 GHz and 5.9 GHz are simulated in Ansys HFSS^{TM} and then they are obtained by Hittite HMC-T2100 synthesized signal generator (10 MHz to 20 GHz) and Krytar® 9000B power meter (100 kHz to 40 GHz) with Krytar® 9530A power sensor (100 kHz to 26.5 GHz). The radiated beams of the proposed antenna at 1.575 GHz and 5.9 GHz are found to be oriented in the broadside direction but at 3.71 GHz, the two major lobes of the antenna beam are tilted by 35° on both sides from the broadside direction as illustrated in Fig. 12. The measured gain of the proposed antenna corresponding to 1.575 GHz and 5.9 GHz at $\phi = 0°$ and $\theta = 0°$ are obtained as 5.3 dBi and 8.5 dBi respectively. At 3.71 GHz, it is found to be 6.5 dBi at $\phi = 0°$ and $\theta = \pm 35°$. The simulated radiation efficiency of the proposed antenna corresponding to 1.575 GHz and 5.9 GHz at $\phi = 0°$ and $\theta = 0°$ are found to be 61.19% and 70.01% respectively. At 3.71 GHz, it is found to be 72.59% at $\phi = 0°$ and $\theta = \pm 35°$.

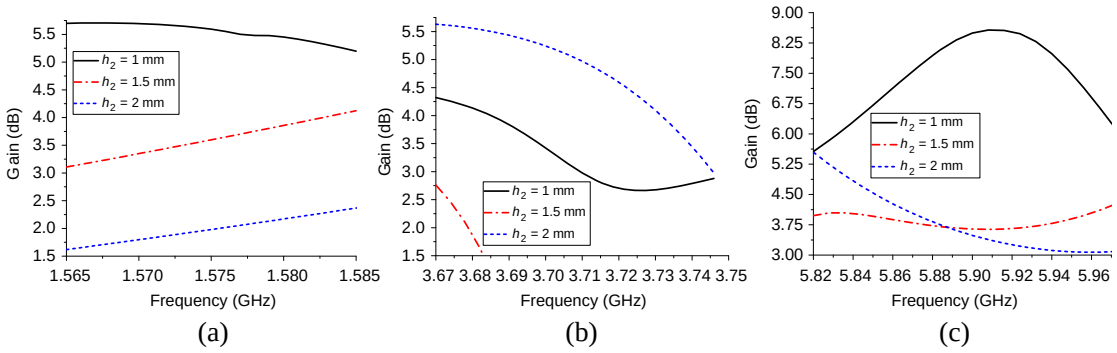

Figure 13. Gain vs. frequency with the variation of air gap h_2. (a) 1.575 GHz. (b) 3.71 GHz. (c) 5.9 GHz.

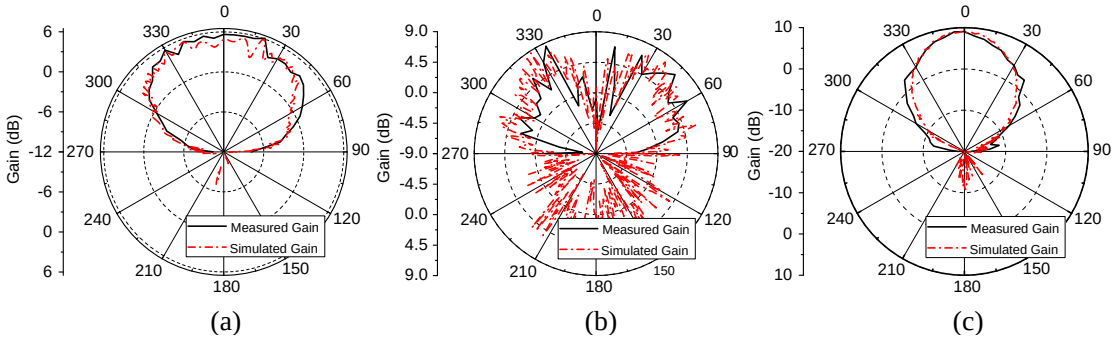

Figure 14. 2D radiation patterns of the antenna mounted on the vehicle (at $\phi = 0°$ plane). (a) 1.575 GHz. (b) 3.71 GHz. (c) 5.9 GHz.

4.3. Variation of the Air Gap in the Proposed Multi-layered Structure

A parametric study has been done by varying the height of the air gap in the proposed multi-layer structure to analyse its effect on the antenna characteristics. In this sense, the height of the air gap h_2 is varied from 1 mm to 2 mm. The variation of gain at the three operating frequency 1.575 GHz, 3.71 GHz and 5.9 GHz with the variation in h_2 are illustrated in Fig. 13. At 1.575 GHz, the gain is found to degrade significantly as h_2 is increased from 1 mm to 2 mm. At 3.71 GHz, the gain improves significantly as h_2 is increased to 2 mm. At 5.9 GHz, relatively high gain is obtained corresponding to 1 mm air gap and it degrades significantly with further increase in h_2. It is observed from the results that the antenna with $h_2 = 1$ mm has the optimum gain at the desired frequency bands.

4.4. On-Vehicle Simulation and Experimentation of the Proposed Fractal Antenna

When the antenna is mounted on the car body, the measured gain values at the three stated frequencies are found to be improved due to the electromagnetic effect of the car as shown in the Fig. 14. The on-vehicle measured gain of the proposed antenna corresponding to 1.575 GHz and 5.9 GHz at $\phi = 0°$ and $\theta = 0°$ are found to be 5.6 dBi and 9.02 dBi respectively. At 3.71 GHz, it is found to be 8.6 dBi at $\phi = 0°$ and $\theta = \pm 35°$. The simulated 3D radiation patterns at the three stated frequencies of the antenna along with the car body are shown in Fig. 15(a), Fig. 15(b) and Fig. 15(c).

4.5. Effect of Adjacent Vehicle as Scattering Object

The effect of the other adjacent cars as scattering objects is studied by placing another car beside the test vehicle. At the operating frequency 1.575 GHz, the gain is noticeably found to improve to 11 dBi

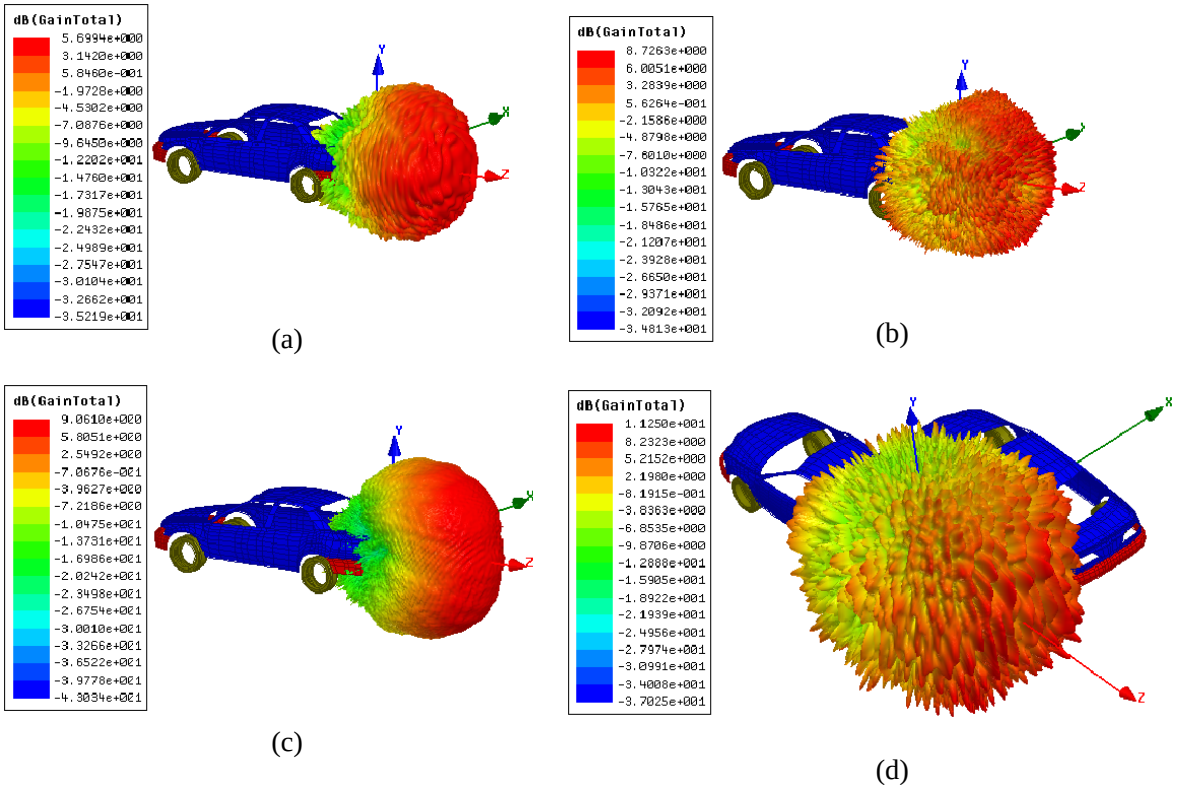

Figure 15. 3D radiation pattern of the antenna mounted on the vehicle. (a) 1.575 GHz. (b) 3.71 GHz. (c) 5.9 GHz. (d) 1.575 GHz with adjacent scattering vehicle.

in the desired direction due to the presence of the adjacent vehicle as another large metallic reflector in the vicinity of the test vehicle as portrayed in Fig. 15(d).

5. CONCLUSION

The proposed tri-band hexagonal fractal antenna reduces the antenna size appreciably by 75% with a minimum compromise in the antenna gain and bandwidth which is actually rendered superior to the performance of other popular fractal designs by the integration of modified Sierpinski fractal with T-shaped slots. The use of the multi-layered structure with electromagnetic feeding technique helps the antenna to achieve high gains at all the three of its operating frequencies in the desired directions. The 3D radiation patterns including over the vehicle body indicate that the electromagnetic radiation inside the car is negligible which makes the antenna electromagnetically compatible with the vehicle. Moreover, as this proposed antenna works well in GPS L1, WiMAX and DSRC bands simultaneously, it can be used in multiple applications of vehicular communication.

ACKNOWLEDGMENT

The research activities have been facilitated by the Advanced Communication Laboratory (developed under the MODROB project funded by All India Council of Technical Education, India; AICTE grant No. 8024/RIFD/MOD-63/2010-11) of the Electronics and Communication Engineering department, Dr. B. C. Roy Engineering College, Durgapur, West Bengal, India. The research work has also been supported by the Microwave and Antenna Research Laboratory, Department of Electronics and Communication Engineering, National Institute of Technology Durgapur, West Bengal, India and the Microwave Measurement and Simulation Laboratory, Department of Electronics and Telecommunication Engineering, IIEST Shibpur, West Bengal, India.

REFERENCES

1. Etou, Y., T. Sugiyama, K. Abe, and T. Abe, "Corner detection using slit rotational edge-feature detector," *2002 IEEE Int. Conf. on Image Processing*, Vol. 2, 797–800, 2002.
2. Alonso, J. D., E. Ros Vidal, A. Rotter, and M. Muhlenberg, "Lane-change decision aid system based on motion-driven vehicle tracking," *IEEE Trans. on Vehicular Technology*, Vol. 57, No. 5, 2736–2746, Sep. 2008.
3. Misnan, M. F., N. H. M. Arshad, R. L. A. Shauri, N. Abd Razak, N. M. Thamrin, and S. F. Mahmud, "Real-time vision based sensor implementation on unmanned aerial vehicle for features detection technique of low altitude mapping," *2013 IEEE Conf. on Systems Process & Control (ICSPC)*, 289–294, Dec. 13–15, 2013.
4. Kuwana, J. and M. Itoh, "Dynamic angling side-view mirror for supporting recognition of a vehicle in the blind spot," *IEEE Int. Conf. on Control, Automation and Systems*, Vol. 2008, 2913–2918, Oct. 14–17, 2008.
5. Leelaratne, R. and R. Langley, "Multiband PIFA vehicle telematics antennas," *IEEE Trans. on Vehicular Technology*, Vol. 54, 477–485, 2005.
6. Best, S. R., "A comparison of the performance properties of the Hilbert curve fractal and meander line monopole antenna," *Microw. Opt. Technol. Lett.*, Vol. 35, No. 4, 258–262, 2002.
7. Gonzalez-Arbes, J. M. and J. Romeu, "Experiences on monopoles with the same fractal dimension and different topology," *IEEE Ant. and Prop. Soc. Int. Symp.*, Vol. 4, 218–222, Jun. 2003.
8. Comisso, M., "On the use of dimension and lacunarity for comparing the resonant behavior of convoluted wire antennas," *Progress In Electromagnetics Research*, Vol. 96, 361–376, 2009.
9. Mandelbrot, B. B., *The Fractal Geometry of Nature*, W. H. Freeman and Company, New York, 1983.
10. Gianvittorio, J. P. and Y. Rahmat-Samii, "Fractal antennas: A novel antenna miniaturization technique, and applications," *IEEE Antennas and Propagation Magazine*, Vol. 44, No. 1, 20–36, Feb. 2002.
11. Puente-Baliarda, C., J. Romeu, R. Pous, and A. Cardama, "On the behavior of the Sierpinski multiband fractal antenna," *IEEE Transactions on Antennas and Propagation*, Vol. 46, No. 4, 517–524, Apr. 1998.
12. Kumar, G. and K. P. Ray, *Broadband Microstrip Antennas*, Artech House, Norwood, MA, 2003.
13. Chaudhary, R. K., V. V. Mishra, K. V. Srivastava, and A. Biswas, "Multi-layer multi-permittivity dielectric resonator: A new approach for improved spurious free window," *2010 European Microwave Conf. (EuMC)*, 1194–1197, Sep. 28–30, 2010.
14. Baliarda, C. P., J. Romeu, and A. Cardama, "The Koch monopole: A small fractal antenna," *IEEE Transactions on Antennas and Propagation*, Vol. 48, No. 11, 1773–1781, Nov. 2000, Doi: 10.1109/8.900236.
15. Krishna, D. D., M. Gopikrishna, C. K. Aanandan, P. Mohanan, and K. Vasudevan, "Compact wideband Koch fractal printed slot antenna," *IET Microwaves, Antennas & Propagation*, Vol. 3, No. 5, 782–789, Aug. 2009, Doi: 10.1049/iet-map.2008.0210.
16. Mahatthanajatuphat, C., S. Saleekaw, P. Akkaraekthalin, and M. Krairiksh, "A rhombic patch monopole antenna with modified minkowski fractal geometry for UMTS, WLAN, and mobile WiMAX application," *Progress In Electromagnetics Research*, Vol. 89, 57–74, 2009.
17. Oraizi, H. and S. Hedayati, "Circularly polarized multiband microstrip antenna using the square and Giuseppe Peano fractals," *IEEE Transactions on Antennas and Propagation*, Vol. 60, No. 7, 3466–3470, Jul. 2012.